Power Line Communication in Automotive Harness on the Example of Local Interconnect Network

Ghyoor Arshad Lodi[*], *Andreas Ott*[†], *Sher Ali Cheema*[*], *Martin Haardt*[*], *and Thomas Freitag*[†]
[*]Communications Research Laboratory
Ilmenau University of Technology, Germany
[†]Melexis GmbH Erfurt, Germany
Email: {Ghyoor-Arshad.Lodi, Sher-Ali.Cheema, Martin.Haardt}@tu-ilmenau.de, andreas.ott@ieee.org

***Abstract*—In recent years, the proliferation of electronic systems in modern cars has resulted in increased cost, complexity, and weight of the automotive wire harness. Moreover, the addition of nodes in to the existing wire harness, to provide additional functions, leads to an enormous routing effort. Power Line Communication (PLC) provides an attractive solution to these problems by providing an alternative medium of communication between the nodes through the vehicle's battery power line. In this work, a new transceiver architecture is proposed to provide PLC on the DC line in an automotive harness. The proposed scheme is based on the example of the Local Interconnect Network (LIN) where only the physical layer is changed. Here, we propose to use redundant transmission channels, which are spaced in frequency, to provide robustness against the severe power line channel attenuation. An improvement in channel gain for the worst-case scenarios is demonstrated through a statistical evaluation of this scheme. The results show that an efficient use of the frequency spectrum enables the support of up to 15 LIN buses on a single power line, while ensuring 3-level redundancy. A system-level design of the PLC system for LIN and its specifications are presented. A further improvement in the system performance in the presence of impulsive noise is demonstrated by applying simple channel coding techniques.**

Keywords – Power Line Communication (PLC), Local Interconnect Network (LIN)

I. Introduction

A variety of electronic systems, that perform several tasks to enhance the driving experience in terms of safety, comfort, and entertainment, are installed in present-day automobiles. These tasks can range from the monitoring of critical real-time information of the engine to non-critical applications such as controlling the side-view mirrors. The electronic modules that control these functions are termed as Electronic Control Units (ECUs). The number of ECUs in cars has increased dramatically over the past years, which has resulted in an increased number of wires in the harness. According to [1], in the near future, the cost of electronics in a medium sized vehicle could amount to as much as 40% of the total cost. The network of these ECUs, also termed as In-Vehicle Network (IVN), provides the backbone for communication and monitoring in automotive electronic systems. The IVNs are deployed with different network topologies according to their use and their requirements such as data volume and data rates.

The weight, cost, and routing complexity of the harness has increased as a consequence of the proliferation in the number of ECUs in modern vehicles. Currently copper wires are used for carrying data signals between different electronic modules within a modern day vehicle. One solution may be to use the battery power line as an alternative medium for communication. This will result in the removal of data-carrying wires which will in return reduce the overall cost, decrease the weight, and decrease the complexity of the harness. In [2] and [3], the issues related to the implementation of PLC in the automotive environment have been explored and presented.

One of the fundamental tasks in designing a PLC system is the study and analysis of vehicular power line communication (VPLC) channels. In this regard, researchers in [4] and [5] have performed S-parameter measurements between different access points for the power nets of two vehicles, to statistically analyze the channel. The measurements were performed on a Lexus RX-350 and a Pontiac Solstice 2006 in [4] and [5], respectively. The source measurement data has been made available to other researchers for further analysis in an on-line database [6], which has been utilized in this work. Moreover, we propose to use 4 parallel frequency spaced channels to enhance the robustness against the severe channel attenuations. The efficacy of the proposed scheme has been evaluated in terms of the channel gain improvement while avoiding the deep notches present in the transfer function of VPLC. The measurements in [4] and [5] are performed over a frequency range of 100 kHz-100 MHz and 500 kHz-100 MHz, respectively. However, for our analysis, we limit the frequency range of interest to 20-30 MHz.

The remainder of the paper is organized as follows: Section II provides an analysis of the measurement results taken from [6] in terms of insertion gains and coherence bandwidth for the frequency range mentioned above. Section III provides the specifications of the proposed PLC system which includes the frequency plan, channel generation, transmitter/receiver architecture, and bus selection mechanism. Section IV deals with the improvement in insertion gain (for the worst-case scenarios) by using the proposed frequency plan. Moreover, the evaluation of the channel coding scheme to improve the system performance is also provided. Conclusions from the work are drawn in Section V.

978-1-4673-6643-4/16/$31.00 ©2016 IEEE

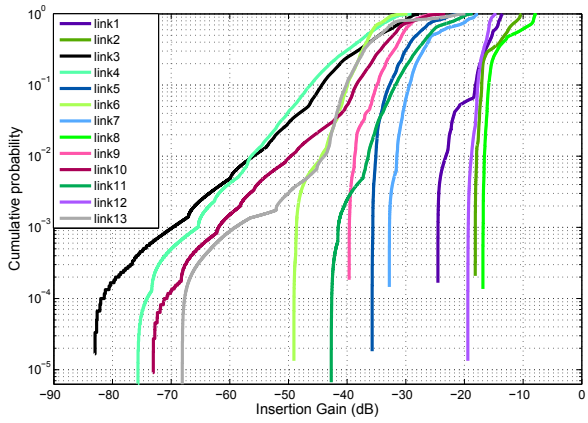

Fig. 1. Cumulative probability of insertion gains of individual links for all states

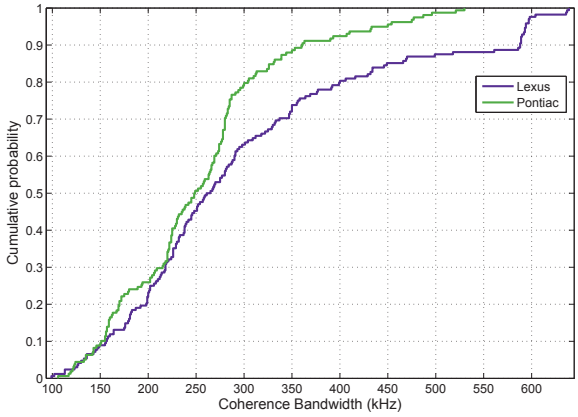

Fig. 2. Cumulative probability of coherence bandwidth for the Lexus RX-350 and the Pontiac Solstice 2006 vehicles

II. Analysis of Measurement Results

The details of the theoretical background for deriving the channel transfer function from S-parameter data is provided in [4]. Considering a matched source, load, and reference impedances, the channel transfer function is given by:

$$H(f) = S_{21}(f) - 6 \qquad \text{(dB)} \tag{1}$$

The data used to analyze the insertion gains in the frequency range of 20-30 MHz is provided in [6] for the Lexus RX-350 vehicle. The measurement data is grouped as links and states of the vehicle. Links refer to the communication path between two access points within the car power net, while states represent the various routines of the driver activity, e.g., position of the key switch or a headlight switch. In total, 13 links and at least 15 different states for each link have been reported [6]. The important observation is that the insertion gain between two access points not only depends on the link, but also varies with different channel states. Another aspect to be highlighted is the fact that the insertion gain plots for the VPLC channels contain deep notches, which must be avoided to ensure reliable communication between nodes. Figure 1 shows the cumulative density function (CDF) of different links in all possible states, in the frequency range of 20-30 MHz.

The analysis of frequency selectivity of VPLC channel is an essential requirement for designing a PLC system for LIN. An important parameter to characterize the frequency selective behavior of the channel is coherence bandwidth (CB). Coherence bandwidth can be defined by the frequency correlation function (FCF) of the complex transfer function H(f) of the channel. The FCF is mathematically defined in [7] as:

$$R(\Delta f) = \int_{-\infty}^{+\infty} H(f)H^*(f+\Delta f)\,df, \tag{2}$$

where, superscript $(\cdot)^*$ denotes the complex conjugate and Δf is the frequency separation between the two points for which the correlation is calculated. Moreover, $R(\Delta f)$ gives the magnitude of the correlation of the channel transfer function at a certain frequency shift Δf. Coherence bandwidth for a particular channel defines the range of frequencies (bandwidth) over which the channel is assumed to have a flat magnitude response (equal gain) and a linear phase response [8]. There is no precise definition for the magnitude of the frequency correlation coefficient that describes the 'flatness' of the channel [7], however values of 0.5, 0.7, and 0.9 are mostly used in the literature. Thus, the coherence bandwidth is always identified by the value of the correlation coefficient for which it is calculated. In this work, the coherence bandwidth is calculated for a frequency correlation coefficient of 0.9, and is denoted by $CB_{0.9}$.

In addition to the measured data for the PLC channels for the Lexus RX 350, the channel measurement data of the Pontiac Solstice from [6] is also used to calculate $CB_{0.9}$ of the PLC channels according to equation (2). The frequency range for this data is 20.5 MHz-30.5 MHz with a frequency shift value of Δf = 1000 Hz. The value of $CB_{0.9}$ is calculated for all channels for all links and all states. It can be observed from Figure 2 that the $CB_{0.9}$ for both vehicles lies in between 100 kHz-700 kHz for all observations. The mean value of the coherence bandwidth comes out to be 301.9 kHz and 254.1 kHz for the Lexus RX 350 and the Pontiac Solstice, respectively.

III. PLC System Specifications

One of the means of preserving the link quality and providing a given Quality of Service (QoS) over the PLC is to adopt redundancy. One way to achieve this is by spreading the signal energy over a wide frequency bandwidth. We can achieve this by applying Direct Sequence Spread Spectrum (DSSS) or Frequency Hopping Spread Spectrum (FHSS). Since LIN is a universal asynchronous receiver/transmitter (UART) based protocol, employing either DSSS or FHSS for the LIN physical layer would require considerable effort in synchronization among communicating nodes. Moreover, as

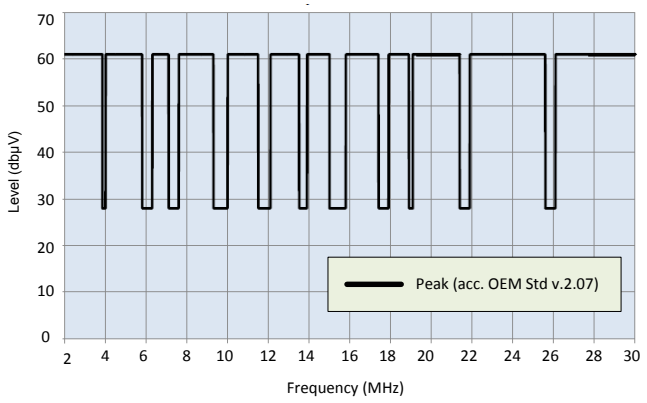

Fig. 3. Emission requirements 2—30 MHz [10]

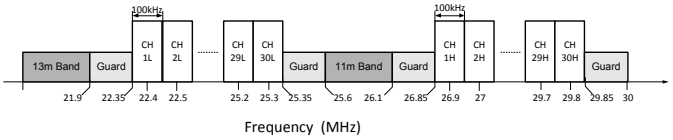

Fig. 4. Frequency plan of 60 channels divided into Low (L) / High (H) bands

LIN targets low-end applications [9], the cost of hardware and implementation is also a key factor which should be taken into account while designing the system. Therefore, a simpler method for employing multiple parallel independent channels is given in this work. This helps to avoid deep notches in the power line transfer function while fulfilling the requirement of redundancy.

A. Frequency Plan

A foremost requirement for the transmission frequency used by the vehicular PLC system is that it should not interfere with other systems operating in the pre-allocated frequency bands. Figure 3 gives an overview of the electromagnetic compatibility (EMC) emission requirements in the frequency range of 2 MHz-30 MHz [10]. Frequencies higher than 30 MHz and their associated higher-order harmonics for in-vehicle PLC could be a cause of interference with the FM radio bands (87.5-108 MHz). It can be observed from Figure 3 that the EMC emission spectrum up to 22 MHz contains many notches which are representative of short-wave (SW) radio bands. However, between 22-30 MHz, the only interferer is the 11m radio band (25.6-26.1 MHz). Therefore, a frequency range from 22-30 MHz has been identified for the transmission while avoiding the 11m radio band.

The identified frequency range of 22-30 MHz can be further divided into two groups of 30 narrowband channels. The two groups of channels are identified as 'low' and 'high' bands, depending on their presence above or below the 11m band in the frequency spectrum, respectively. Each channel is 100 kHz wide and the adjacent channel separation within each low/high band is also 100 kHz. As stated in Section II, the vehicular PLC channel's coherence bandwidth was found to be greater than 100 kHz for all scenarios. A channel bandwidth of 100 kHz, which is less than the minimum $CB_{0.9}$ would imply that the signal sent over the PLC channel would experience flat-fading [11]. This would imply that the receiver design for such communication would not require a frequency-domain equalization technique, thus simplifying the hardware requirements. Small phase and gain errors in the absence of an equalizer would not degrade the overall system performance.

TABLE I
FREQUENCY PLAN FOR ALL 60 CHANNELS AND CORRESPONDING BUS NUMBERS

Bus No.	Channel No.	Frequencies (MHz)			
1	1L, 16L, 1H, 16H	22.4	23.9	26.9	28.4
2	2L, 17L, 2H, 17H	22.5	24.0	27.0	28.5
3	3L, 18L, 3H, 18H	22.6	24.1	27.1	28.6
4	4L, 19L, 4H, 19H	22.7	24.2	27.2	28.7
5	5L, 20L, 5H, 20H	22.8	24.3	27.3	28.8
6	6L, 21L, 6H, 21H	22.9	24.4	27.4	28.9
7	7L, 22L, 7H, 22H	23.0	24.5	27.5	29.0
8	8L, 23L, 8H, 23H	23.1	24.6	27.6	29.1
9	9L, 24L, 9H, 24H	23.2	24.7	27.7	29.2
10	10L, 25L, 10H, 25H	23.3	24.8	27.8	29.3
11	11L, 26L, 11H, 26H	23.4	24.9	27.9	29.4
12	12L, 27L, 12H, 27H	23.5	25.0	28.0	29.5
13	13L, 28L, 13H, 28H	23.6	25.1	28.1	29.6
14	14L, 29L, 14H, 29H	23.7	25.2	28.2	29.7
15	15L, 30L, 15H, 30H	23.8	25.3	28.3	29.8

An overview of the breakdown of the frequency range into individual channels, along with additional guard bands to limit out-of-band emissions, is shown in Figure 4. A detailed channel assignment for each LIN bus is given in Table I.

The main motivation behind the division of the available frequency range into a large number of channels is to enable the function of multiple LIN buses on the same power line and to provide redundancy. In the case where four out of 60 independent channels are assigned to each LIN bus, a total of 15 independent LIN buses could be theoretically supported on a single power line. Out of each group of 4 channels assigned to a specific LIN bus, 2 channels from each high/low band are selected. Channels within the same band are separated by 1.5 MHz and those between different bands by 4.5 MHz. This separation in frequency provides protection against deep notches in the transfer function of the PLC channel, as shown in Section IV. Each of the 60 channels are identified with a channel number (1-30) and the corresponding band (L or H).

B. Generation Scheme for Redundant Channels

Channel generation and translation may be characterized in to 3 steps. The first two steps generate 4 side-bands around zero-frequency with required frequency spacing. The third step shifts the generated sidebands to the required RF frequency. An illustration of the 3-step channel conversion is given in Figure 5. The steps can be summarized as follows:

1) Mixing of base-band signal with the local oscillator (LO_3) operating at f_{LO3} = 0.75 MHz. This shifts the baseband spectrum at $\pm$ 0.75 MHz around zero-frequency.

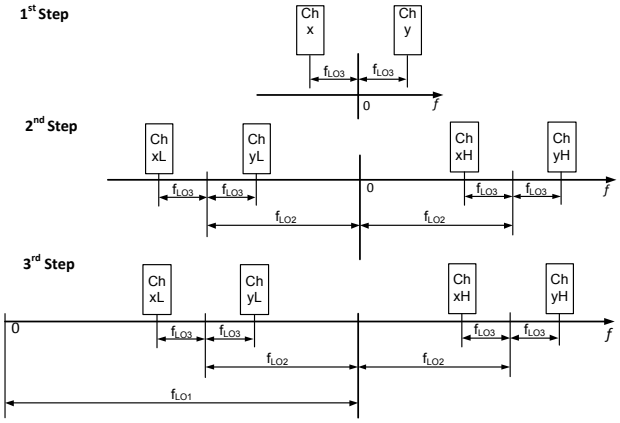

Fig. 5. 3-Step conversion to generate 4 channels

2) Further mixing of the output signal of LO_3 is done by the local oscillator (LO_2) operating at f_{LO2} = 2.25 MHz. This creates the signal which has 4 spectral components at $\pm$ 1.5 MHz and $\pm$ 3 MHz around DC (zero frequency).
The 4 copies of the baseband signal are centered at the following frequencies:

- f_{LO3} + f_{LO2} = +3.0 MHz
- -f_{LO3} + f_{LO2} = +1.5 MHz
- f_{LO3} - f_{LO2} = -1.5 MHz
- -f_{LO3} - f_{LO2} = -3.0 MHz

3) Lastly, shifting of the group of 4 spectral components centered at DC to the RF frequency is done by the local oscillator (LO_1) which operates at a variable frequency f_{LO1}. To create a 100 kHz channel spacing between adjacent channels in the frequency plan, the value of f_{LO1} is varied by 100 kHz for successive bus numbers. The value f_{LO1} is calculated by the following relation:

$$f_{LO1}(n) = f_i + (N \times 10^5) \quad \text{(Hz)} \tag{3}$$

Where, f_i = 25.4 MHz, n is the bus number ranging from 1 to 15 and $N = n - 1$.

C. Modulation Scheme

The scheme chosen for the modulation of binary data is Gaussian-Minimum-Shift-Keying (GMSK), a variant of the Minimum-Shift-Keying (MSK). GMSK is a well-known modulation technique used in the Global System for Mobile Communications (GSM) standard. In GMSK the Non-Return-to-Zero (NRZ) binary data is passed through a pre-modulation Gaussian pulse shaping filter which reduces the side-lobe levels of the spectrum [11]. The Gaussian pulse shaping applied at the baseband smooths the sudden frequency variations over time and subsequently reduces the side-lobe level. Furthermore, the GMSK modulated signal has a constant envelope in time, which is a big benefit in terms of power efficiency when used with non-linear class-C power amplifiers [11].

The spectrum of GMSK modulation is defined by the product of the 3-dB bandwidth of the Gaussian filter and the bit duration, i.e., BT. Reducing the value of BT reduces the side-lobe levels. However, reducing the value of BT also increases the Inter-Symbol-Interference (ISI) which degrades the performance of the communication scheme [12]. Therefore, an optimal trade-off between the performance degradation (in terms of SNR) and the increased spectral efficiency must be reached. For the proposed design of the system, a value of BT = 0.3 is identified.

Simulations results show that with a value of BT = 0.3 and a bit rate of 20 kbit/s, 99.9% of the RF power of the GMSK modulated signal is contained within a 32 kHz bandwidth. This also provides sufficient guard space to limit adjacent channel interference (ACI), as the proposed system uses adjacent channel spacing of 100 kHz.

D. Transmitter Architecture

The transmitter along with the required signal processing stages is shown in Figure 6. As described in Section III-B, LO_3 and LO_2 have an oscillating frequency of 0.75 MHz and 2.25 MHz, respectivley. The implementation of these mixing stages is proposed to be in digital domain, operating at a sampling rate of $4f_{LO}$. This reduces the sinusoidal signal of the local oscillator to a repeating sequence of [0 1 0 -1]. The advantage of this technique is that the local oscillator can be implemented through a digital multiplexer (MUX), where the MUX input is sequentially selected at the respective sampling rate. Moreover, the mixing is done with a complex mixer, which avoids the problem of image frequency.

Before the first mixing stage, the input signal needs to be up-sampled to 3 MS/s and then low-pass filtered. The input data rate at the modulator input is 20 kbit/s. Therefore, an interpolation factor $L_1 = 150$ is required. Similarly, the output signal from the 1st mixing stage needs to be up-sampled to 9 MS/s and low-pass filtered before being fed as the input to the second mixing stage. The required interpolation factor L_2 in the intermediary stage between the first and second mixing stage is 3.

The final up-conversion stage to RF is proposed to be implemented in the analog domain. This is performed by a one-sided local oscillator $e^{j2\pi f_{LO1}t}$ at mixing stage 3. Due to the non-idealities of the analog quadrature mixers, such as the mismatch in amplitude and phase between I and Q path, ideal one-sided frequency translation is not possible. Some residual components centered at -f_{LO1} appear, which must be suppressed before transmission. To suppress the signal components on the negative side of the spectrum, a poly-phase filter (PPF) [13] which has asymmetric frequency response for positive and negative frequency components can be used. Use of complex filtering is also needed to limit out-of-band emissions during transmission.

In the case where there is a need to increase the total number of supported LIN buses, the level of redundancy could

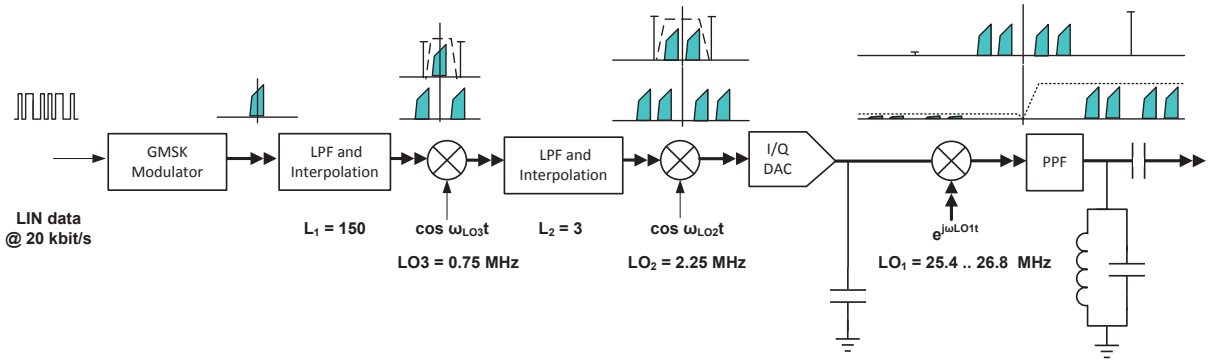

Fig. 6. Transmitter architecture with 3 redundant channels for each LIN bus

be reduced. This would require independent modulation of digital data at the baseband, shifting the generated baseband signals around DC and then adding them before the final up-conversion. The required interpolation stages in case of lower-level redundancy (0 or 1 redundant channel) would increase. The decision about the level of redundancy can thus be taken at system-level.

E. Receiver Architecture

The stages in the receiver are reciprocal to the transmitter stages. The receiver processes each of the four received channels over the power line independently, regardless of the level of redundancy. So, all four received channels are converted to the baseband to be independently demodulated by the GMSK demodulator. A non-coherent demodulator is proposed in this work. The demodulation of all four channels at the baseband produces 4 independent bit-streams which are combined through a bit-decision algorithm. In this system a simple 4-vote majority decision decoding algorithm is proposed [14].

For each combination of four input bit-streams 'A', 'B', 'C', and 'D', there is a value of the decoded bit 'H' depending on the number of '0s' or '1s' in majority. In Boolean algebraic notation the output bit 'H' can be expressed in the 'sum of products form' using logical operators as shown in equation (4), which can be implemented with minimal hardware.

$$H(A,B,C,D) = \Big[(\bar{A}BCD) + (A\bar{B}CD) + (AB\bar{C}D) + (ABC\bar{D}) + (ABCD)\Big] \quad (4)$$

For a system with 1 redundant channel, other signal combining techniques such as equal gain combining or maximal ratio combining could be used before the demodulation stage.

The frequency plan given in Table I is evaluated for the measured channel data of 13 links shown in Figure 1. From a group of 15 available groups of four channels each, a unique Bus number is assigned to every link. This will help to improve the efficacy of the proposed frequency plan by avoiding the deep notches present in the transfer function of different links. This will also help to evaluate the performance of the proposed frequency plan in terms of the channel gain improvement, as in a real scenario multiple LIN buses are connected to the same power line.

F. Mechanism for Bus Selection

As shown in Figure 1, each link can have different states depending on the configuration of loads connected to the power line at that instant. Insertion gain from all possible states is combined for each link and the probability of insertion gain experienced by different groups of four channels, represented by a unique bus number, is evaluated. The assignment of a bus number to a particular link is permanent. Therefore, a mechanism must be decided by which the bus number are assigned so that deep notches in the transfer function could be avoided. The assigning of bus number works on the following metrics:

1) The link having the minimum value of insertion gain (worst link) is considered first and channels from all 15 buses are evaluated.

2) The bus number which has the maximum insertion gain as compared to the other buses is permanently assigned to the link. The next link is evaluated from remaining 14 buses, and so on.

IV. Improvement in System Performance

A. Improvement in Channel Gains

Figure 7 gives a comparative overview of the improvement in the channel attenuation after the optimal assignment of buses to individual links. It can be observed that the proposed frequency plan serves its purpose of utilizing the available spectrum efficiently and avoiding deep notches in the transfer function of the PLC channel. For example, link 3, which exhibits a high channel attenuation of 84 dB will experience a significant gain improvement (42 dB) if the channel frequencies of bus number 15, i.e., 23.8 MHz, 25.3 MHz, 28.3 MHz, and 29.8 MHz are assigned. Similarly, the gains for all links with high attenuations are improved.

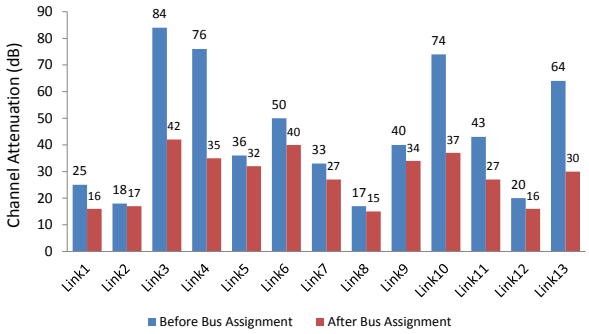

Fig. 7. Improvement in channel attenuation after optimal assignment of buses

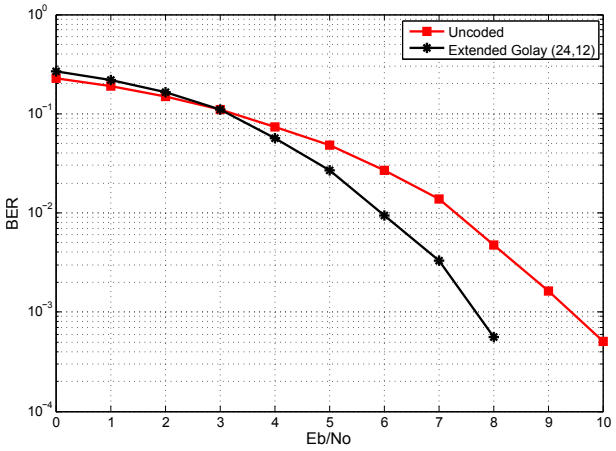

Fig. 8. Performance of extended binary Golay coding over AWGN

For this study, the frequency plan is evaluated on the measurement data of Lexus RX-350. However, after obtaining sufficient measurement data for different links within the power net, the frequency plan can be evaluated on any vehicle and the channel frequencies can be assigned to specific LIN buses.

B. Performance Improvement through Channel Coding

To add robustness against impulse noise, the channel coding techniques can be applied. As the channels in our proposed scheme are 100 kHz apart, a low coding rate would require an increased signal bandwidth which would subsequently result in an increased adjacent channel interference. Also, the hardware requirements of the coding scheme must not be high as the PLC system designed for LIN targets low-end and non-critical applications. While keeping in view these requirements, extended binary Golay code [15] $(n, k, d_{\min})$ = (24,12,8) has been identified as a possible candidate. The BER performance of the extended binary Golay coding in an additive white Gaussian noise (AWGN) channel was evaluated using Matlab. It can be seen from Figure 8 that introducing channel coding into the system results in an improved performance.

V. Conclusion

The main focus of this work was to explore the possibility of PLC in the automotive wire harness based on the example of LIN. A new PLC scheme with its required specifications was proposed in this work. To avoid deep notches in the channel transfer function, a transmission using 4 parallel channels, separated in frequency, was recommended. The evaluation of this technique on an open-source measurement data set belonging to a Lexus RX 350 was performed. It was found that using 4 parallel frequency channels result in avoiding deep notches in the channel transfer function and hence considerably improves the channel gains for the worst-case scenarios. The other benefits of the proposed PLC system for LIN is the support of up to 15 individual LIN buses on a single power line, which can consequently support a large number of LIN nodes. This provides ease of scalability to the existing LIN networks in the automotive harness.

Currently, no standard exists in the automotive sector for the specification of PLC modems for LIN. This work could prove to be a basis for further research in this domain and eventual standardization of PLC specifications for LIN in automotive scenario.

References

[1] S. D. Caro, A. Testa, and R. Letor, "Power Line Communication Approach for Body Electronics Modules", in *European Conference on Power Electronics and Applications, (EPE)*, Barcelona, Sep. 2009, pp. 1–10.

[2] F. Benzi, T. Facchinettia, and T. Nolte, "Towards the Powerline Alternative in Automotive Applications", in *IEEE International Workshop on Factory Communication Systems, (WFCS)*, 2008.

[3] F. Nouvel, and P. Tanguy, "What is about future high speed power line communication systems for in-vehicles networks?", in *Information, Communications and Signal Processing (ICICS)*, Macau, China, Dec. 2009, pp. 1-6.

[4] N. Bahrani and V. Gaudet, "Measurements and Channel Characterization for In-Vehicle Power Line Communications", in *IEEE Intl. Symposium on Power Line Commun. and its Appl. (ISPLC)*, Glasgow, Scotland, Mar. 2014, pp.64–69.

[5] M. Mohammadi, L. Lampe, M. Lok, S. Mirabbasi, M. Mirvakili, R. Rosales, and P. van Veen, "Measurement Study and Transmission for In-vehicle Power Line Communication", in *IEEE Intl. Symposium on Power Line Commun. and its Appl. (ISPLC)*, Dresden, Germany Mar. 2009. pp.73-78.

[6] "In-Vehicle Power Line Communication Project.", [online] "http://ivplc.ece.ubc.ca/" (last accessed: Sep. 2015).

[7] M. Tlich, A. Zeddam, F. Moulin, and F. Gauthier, "Indoor Power-Line Communications Channel Characterization up to 100 MHz—Part II: Time-Frequency Analysis", in *IEEE Trans. Power Delivery*, vol. 23, no. 3, pp.1402–1409, Jul. 2008.

[8] V. J. Arokiamary, "*Mobile Communications*", 1st ed., Technical Publications Pune, 2009.

[9] "*LIN Specification Package Rev. 2.2a*", Dec. 2010, [online] "www.lin-subbus.org"

[10] "Electromagnetic Compatibility (EMC) Requirement (strip-line test)"acc. to Harmonized OEM Standard v. 2.07.

[11] T. S. Rappaport, "*Wireless Communications: Principles and Practice*", 2nd ed. Prentice Hall Inc. 2002.

[12] K. Mupota, and K. Hirade, "GMSK Modulation for Digital Mobile Radio Telephony", in *IEEE Trans. on Commun.,* vol. Com-29, no. 7, Jul. 1981.

[13] J. Crols, and M. Steyaert, "CMOS Wireless Transceiver Design", Kluwer Academic Publishers, 1997.

[14] A. Neubauer, J. Freudenberger, and V. Kühn, "Coding Theory Algorithms, Architecture and Applications", John Wiley & Sons, 2007.

[15] R. H. Morelos-Zaragoza, "The Art of Error Correcting Coding: Chapter 2, Page 30", 2nd ed., John Wiley & Sons, 2006.